



Published in final edited form as:

Cell. 2010 October 29; 143(3): 390–403. doi:10.1016/j.cell.2010.09.049.

The long noncoding RNA, *Jpx*, is a molecular switch for X-chromosome inactivation

Di Tian, Sha Sun, and Jeannie T. Lee*

Howard Hughes Medical Institute, Department of Molecular Biology, Massachusetts General Hospital, Department of Genetics, Harvard Medical School, and Department of Pathology, Massachusetts General Hospital

SUMMARY

Once protein-coding, the X-inactivation center (*Xic*) is now dominated by large noncoding RNAs (ncRNA). X-chromosome inactivation (XCI) equalizes gene expression between mammalian males and females by inactivating one X in female cells. XCI requires *Xist*, a ncRNA that coats the X and recruits Polycomb proteins. How *Xist* is controlled remains unclear but likely involves negative and positive regulators. For the active X, the antisense *Tsix* RNA is an established *Xist* repressor. For the inactive X, here we identify *Xic*-encoded *Jpx* as an *Xist* activator. *Jpx* is developmentally regulated and accumulates during XCI. Deleting *Jpx* blocks XCI and is female-lethal. Posttranscriptional *Jpx* knockdown recapitulates the knockout, while supplying *Jpx in trans* rescues lethality. Thus, *Jpx* is *trans*-acting and functions as ncRNA. Furthermore, ΔJpx is rescued by truncating *Tsix*, indicating an antagonistic relationship between the ncRNAs. We conclude that *Xist* is controlled by two RNA-based switches – *Tsix* for *Xa*, and *Jpx* for *Xi*.

INTRODUCTION

In the mammal, X-chromosome inactivation (XCI) achieves dosage balance between the sexes by transcriptionally silencing one X-chromosome in the female (Lyon, 1961; Luchesi et al., 2005; Wutz and Gribnau, 2007; Payer and Lee, 2008; Starmer and Magnuson, 2009). During XCI, ~1000 genes on the X are subject to repression by the X-inactivation center (*Xic*) (Brown et al., 1991). Multiple noncoding genes have been identified within this 100- to 500-kb domain that, until ~150 million years ago, was dominated by protein-coding genes. The rise of Eutherian mammals and the transition from imprinted to random XCI led to region-wide “pseudogenization” (Duret et al., 2006; Davidow et al., 2007; Hore et al., 2007; Shevchenko et al., 2007). To date, four *Xic*-encoded noncoding genes have been ascribed function in XCI, including *Xist*, *Tsix*, *Xite*, and *RepA* (Brockdorff et al., 1992; Brown et al., 1992; Lee and Lu, 1999; Ogawa and Lee, 2003; Zhao et al., 2008)(Fig. 1A). The dominance of ncRNAs brought early suspicion that long transcripts are favored by allelic regulation during XCI and imprinting (reviewed in (Wan and Bartolomei, 2008; Koerner et al., 2009; Lee, 2009; Mercer et al., 2009)). Indeed, the *Xic* region harbors many other ncRNA (Simmler et al., 1996; Chureau et al., 2002), but many have yet to be characterized.

*corresponding author: lee@molbio.mgh.harvard.edu.

Publisher's Disclaimer: This is a PDF file of an unedited manuscript that has been accepted for publication. As a service to our customers we are providing this early version of the manuscript. The manuscript will undergo copyediting, typesetting, and review of the resulting proof before it is published in its final citable form. Please note that during the production process errors may be discovered which could affect the content, and all legal disclaimers that apply to the journal pertain.

One key player is *Xist*, a 17-kb ncRNA that initiates XCI as it spreads along the X *in cis* (Brockdorff et al., 1992; Brown et al., 1992; Penny et al., 1996; Marahrens et al., 1997; Wutz et al., 2002) and recruits Polycomb repressive complexes to the X (Plath et al., 2003; Silva et al., 2003; Schoeftner et al., 2006; Zhao et al., 2008). In embryonic stem (ES) cell models that recapitulate XCI during differentiation *ex vivo*, *Xist* expression is subject to a counting mechanism that ensures repression in XY cells and monoallelic upregulation in XX cells. Prior to differentiation, *Xist* is expressed at a low basal level but is poised for activation in the presence of supernumerary X-chromosomes (XX state). In the presence of only one X (XY), *Xist* becomes stably silenced.

It has been proposed that *Xist* is under both positive and negative control (Lee and Lu, 1999; Lee, 2005; Monkhorst et al., 2008). Negative regulation is achieved by the antisense gene, *Tsix*. When *Tsix* is deleted or truncated, the *Xist* allele *in cis* is derepressed (Lee and Lu, 1999; Lee, 2000; Luikenhuis et al., 2001; Sado et al., 2001; Stavropoulos et al., 2001; Morey et al., 2004; Vigneau et al., 2006; Ohhata et al., 2008). *Tsix* represses *Xist* induction by several means, including altering the chromatin state of *Xist* (Navarro et al., 2005; Sado et al., 2005; Sun et al., 2006; Ohhata et al., 2008), deploying Dnmt3a's DNA methyltransferase activity (Sado et al., 2005; Sun et al., 2006), recruiting the RNAi machinery (Ogawa et al., 2008), and interfering with the ability of *Xist* and RepA RNA to engage Polycomb proteins (Zhao et al., 2008). In turn, *Tsix* is regulated by *Xite*, a proximal noncoding element that interacts with *Tsix*'s promoter (Tsai et al., 2008) and sustains *Tsix* expression on the future Xa (active X) (Ogawa and Lee, 2003).

Significantly, whereas a *Tsix* deletion has major effects on *Xist* in XX cells, it has little consequence in XY cells (Lee and Lu, 1999; Ohhata et al., 2006). This difference led to the idea that *Xist* is not only negatively regulated on Xa but also positively controlled on Xi (inactive X) by factors that activate *Xist* (Lee and Lu, 1999). Positive regulation finds support in that RepA – a short RNA embedded within *Xist* – recruits Polycomb proteins to facilitate *Xist* upregulation (Zhao et al., 2008; Hoki et al., 2009). Activators outside of the *Xist-Tsix-Xite* region must also occur, as an 80-kb transgene carrying only these genes cannot induce XCI (Lee et al., 1999b). Furthermore, female cells carrying a heterozygous deletion of *Xist-Tsix-Xite* still undergo XCI, indicating female cells with only one copy of *Xist*, *Tsix*, and *Xite* still count two X-chromosomes (Monkhorst et al., 2008). One such activator has been proposed to be the E3 ubiquitin ligase, Rnf12, whose gene resides ~500-kb away from *Xist* (Jonkers et al., 2009). Overexpression of Rnf12 ectopically induces *Xist* expression in XY cells, but Rnf12 is not required for *Xist* activation in XX cells, as its knockout delays but does not abrogate expression. This implies that essential *Xist* activator(s) must reside elsewhere.

Here we seek to identify that essential factor. We draw hints from an older study demonstrating that, while transgenes carrying only *Xist-Tsix-Xite* cannot activate *Xist*, inclusion of sequences upstream of *Xist* restores *Xist* upregulation (Lee et al., 1999b). The Eutherian-specific noncoding gene, *Jpx/Enox* (Chureau et al., 2002; Johnston et al., 2002; Chow et al., 2003), lies ~10-kb upstream of *Xist*, is transcribed in the opposite orientation (Fig. 1A), but remains largely uncharacterized. *Jpx* lacks open reading frames but is relatively conserved in its 5' exons. Initial reports indicate that *Jpx* is neither developmentally regulated nor sex-specific and is therefore unlikely to regulate XCI (Chureau et al., 2002; Johnston et al., 2002; Chow et al., 2003). Although they imply a pseudogene status, chromosome conformation capture (3C) suggests that *Jpx* resides within *Xist*'s chromatin hub (Tsai et al., 2008). We herein study *Jpx* and uncover a crucial role as ncRNA in the positive arm of *Xist* regulation.

RESULTS

Jpx escapes XCI and is upregulated during ES cell differentiation

We first analyzed *Jpx* expression patterns in ES cells, as an *Xist* inducer might be expected to display developmental specificity correlating with the kinetics of XCI. Time-course measurements of *Jpx* and *Xist* during ES differentiation into embryoid bodies (EB) showed that *Jpx* RNA levels increased 10- to 20-fold between d0 and d12 and remained elevated in somatic cells (Fig. 1B and data not shown). Upregulation occurred in both XX and XY cells. However, whereas *Xist* induction paralleled *Jpx* upregulation in female cells, *Xist* remained suppressed in male cells (Fig. 1C). To determine whether *Jpx* originated from Xa or Xi, we carried out allele-specific analysis in *Tsix*^{TST/+} female cells, which are genetically marked by a *Tsix* mutation that invariably inactivates the mutated X of 129 origin (X¹²⁹) instead of the wildtype *Mus castaneus* X (X^{cas}) (Ogawa et al., 2008). On the basis of a Nla-III polymorphism, RT-PCR demonstrated that both alleles of *Jpx* could be detected from d0–d12, indicating that *Jpx* escapes XCI (Fig. 1D). On d0, there was nearly equal expression from both alleles; between d12–d16, expression from Xi accounted for 10–35% of total *Jpx*.

RNA fluorescence in situ hybridization (FISH) showed that 98% of cells expressed *Xist* clouds, and *Jpx* RNA was present on Xi in 60% (Fig. 1E, n=61). In such cells, *Jpx* RNA was seen on both Xa and Xi. On Xi, *Jpx* RNA was always adjacent to, not in, the *Xist* cloud, a juxtaposition characteristic of genes that escape XCI (Clemson et al., 2006; Namekawa et al., 2010). Thus, consistent with previous analysis (Chureau et al., 2002; Johnston et al., 2002; Chow et al., 2003), our results indicate ubiquitous, non-sex-specific *Jpx* expression. However, our data demonstrate that *Jpx* upregulation is developmentally regulated to correlate with *Xist* upregulation, and that *Jpx* significantly escapes XCI.

Deleting *Jpx* has no effect on male cells but is female-lethal

To test *Jpx* function, we knocked out a 5.17-kb region at the 5' end of *Jpx* that includes its major promoter, CpG island, and first two exons (ΔJpx , Fig. 2A, S1A). We isolated four independently derived male ES clones and confirmed homologous targeting by Southern analysis using external and internal probes (Fig. S1B and data not shown). The *Neo* selectable marker was thereafter removed by Cre-mediated excision. Following DNA FISH to verify the deletion (Fig. S1C), we analyzed two independent *Neo*⁻ clones for each. Because 1C4 and 1D4 male clones behaved identically, we present data for 1C4 below.

$\Delta Jpx/Y$ ES cells displayed no obvious phenotype when differentiated into EB to induce XCI. Differentiation in suspension culture from d0–d4 (day 0 to 4) revealed no morphological anomalies, and adherent outgrowth on gelatin-coated plates after d4 yielded robust growth (Fig. S1D). Consistent with this, no elevation of cell death was detected (Fig. S1E). RT-PCR analysis showed that *Xist* was appropriately suppressed during differentiation (Fig. S1F), RNA FISH confirmed that basal *Xist* expression became repressed (Fig. S1G). Furthermore, the X-linked genes, *Pgk1*, *Mecp2*, and *Hprt*, were all expressed appropriately (Fig. S1F, G). Strand-specific qRT-PCR showed that *Xist* and *Tsix* levels in mutants were not significantly different from those of wildtype cells on d0 (Fig. S1H). We conclude that deleting *Jpx* has no functional consequence for XY cells.

We also deleted *Jpx* in a hybrid female ES line (16.7) carrying X-chromosomes of different strain origin (X¹²⁹/X^{cas}) (Lee and Lu, 1999). We isolated five independent female clones, verified homologous targeting by Southern analysis using external and internal probes (Fig. 2A, B and data not shown), and then removed the *Neo* marker by Cre-mediated excision. Allele-specific analysis showed that, in all five cases, X¹²⁹ was targeted (Fig. 2B), consistent with the targeting vector's 129 origin. Following DNA FISH to confirm the deletion (Fig. 2C), we analyzed two independent *Neo*⁻ clones, 1F3 and 1F8. RNA/DNA

FISH showed that >95% of mutant cells are XX throughout differentiation. The two female clones behaved similarly.

To quantitate residual *Jpx* levels in $\Delta Jpx/+$ cells, we performed qRT-PCR and found less RNA than expected (Fig. 2D). On d0, targeting of a single allele resulted in loss of approximately half of *Jpx* RNA, as expected. However, during differentiation, *Jpx* levels from the wildtype *castaneus* allele did not increase to the extent anticipated. Between d8–d16, *Jpx* was expressed at only 10–20% of wildtype levels (50% expected). This disparity could not be explained by strain-specific differences, as allele-specific analysis of wildtype cells demonstrated similar allelic levels between d0–d12 (Fig. 1D). Deleting one *Jpx* allele therefore resulted in effects on the homologous allele, suggesting an expression feedback loop. Thus, a heterozygous deletion severely compromises overall *Jpx* expression and approximates a homozygous deletion.

To investigate effects on XCI, we differentiated ES cells into EB to induce XCI. Although $\Delta Jpx/+$ and wildtype cells were indistinguishable on d0, differentiation uncovered profound effects. Wildtype EB typically showed smooth and radiant borders between d2–d4 when grown in suspension, but mutant EB exhibited necrotic centers, irregular edges, and disaggregation (Fig. 2E, arrows). The difference became more obvious during the adherent phase (post-d4). Whereas wildtype EB adhered to plates and displayed exuberant cellular outgrowth, mutant EB attached poorly and showed scant outgrowth. The difference was not due to *Jpx* effects on cell differentiation *per se*, as immunostaining of stem cell markers showed that mutant EB appropriately downregulated Oct4 and Nanog upon differentiation (Fig. S2). Thus, whereas ΔJpx had little effect in males, deleting one *Jpx* allele in females caused severe abnormalities during differentiation.

The female-specific nature suggested a link to XCI, a process tightly coupled to cell differentiation (Monk and Harper, 1979; Navarro et al., 2008; Donohoe et al., 2009). To test this possibility, we performed a time-course analysis of Xist expression by RNA FISH (Fig. 2F, G). In wildtype cells, XCI was largely established by d8–d12, with $75.0 \pm 4.8\%$ (mean \pm S.E.) of female cells displaying large Xist clusters by d8 and $89.1 \pm 3.4\%$ by d12. However, in $\Delta Jpx/+$ cells, Xist upregulation was severely compromised, with only $6.35 \pm 1.77\%$ displaying Xist foci on d8 and no major increase on d12. Strand-specific RNA FISH confirmed that large RNA clouds during differentiation were of Xist origin and residual pinpoint signals were of Tsix (Fig. S3). The Xist deficiency mirrored poor EB growth and massive cell death over the same time course (Fig. 2E, G). The disparity was greatest between d4–d12, when mutant cell death approached 10-times that of wildtype cells (Fig. 2H). Between d4–d12, at least 85% of mutant cells were lost. Because dead cells detached from culture, the actual percentage of Xist⁺ cells was probably even lower ($\ll 6\%$) than measurable by collecting attached cells for RNA FISH.

Our data argue that *Jpx* is an activator of *Xist*. ΔJpx differs from *Rnf12*, which merely delays *Xist* induction by two days and does not prevent XCI (Jonkers et al., 2009). We believe that ΔJpx blocks XCI rather than delays it, because Xist clouds were rare up to d16. Whereas $\Delta Rnf12/+$ cells are fully capable of expressing Xist, $\Delta Jpx/+$ cells have severely compromised Xist expression at all timepoints. Moreover, whereas $\Delta Rnf12/+$ cells are viable, $\Delta Jpx/+$ cells undergo massive cell death during differentiation. Therefore, *Jpx* serves an essential function and precludes Xist induction when deficient.

Jpx acts in trans

Interestingly, ΔJpx 's influence on *Xist* was not restricted *in cis* to X¹²⁹ but also blocked *Xist* upregulation on X^{cas}, implying that, unlike other *Xic*-encoded factors, *Jpx* may be transacting. If so, expressing *Jpx* from an autosomal transgene might rescue $\Delta Jpx/+$ cells. To

test this, we introduced a 90-kb BAC carrying full-length *Jpx* (and no other intact gene; Fig. 3A) into $\Delta Jpx/+$ cells (1F8) and characterized two independent clones, *Jpx+/-*;TgB2 and *Jpx+/-*;TgB3. Both clones carried autosomal insertions, and qPCR using primer pairs at different transgene positions indicated that each clone carried 1–2 copies of the full-length transgene (Fig. 3B and data not shown). In both clones, *Jpx* levels were restored between d0–d12 (Fig. 3C).

Significantly, both clones behaved differently from $\Delta Jpx/+$ cells and were more similar to wildtype cells. Whereas $\Delta Jpx/+$ cells differentiated poorly and displayed elevated cell death, *Jpx+/-*;TgB2 and *Jpx+/-*;TgB3 cells differentiated well and were fully viable (Fig. 3D, E). Moreover, *Xist* expression was fully restored in *Jpx+/-*;TgB2 and *Jpx+/-*;TgB3 cells, both in steady state levels and in the number of cells with *Xist* clouds (Fig. 3F–H). We conclude that an autosomal *Jpx* transgene rescues the X-linked *Jpx* deletion and that *Jpx* must therefore be able to act *in trans*.

***Jpx* acts as a long ncRNA**

In principle, *Jpx* could function as a positive regulator in several ways. *Jpx* could operate as enhancer, given 3C analysis showing interaction between *Jpx* and *Xist* within a defined chromatin hub (Tsai et al., 2008). However, a luciferase reporter assay in stably transfected female ES cells uncovered no obvious enhancer within the deleted *Jpx* region (Fig. S4). In this assay, *Jpx* not only failed to enhance luciferase expression but actually depressed it in some cases. A relative increase in expression occurred between d0 and d2, but activation never exceeded that of the *Xist*-only construct. While we cannot exclude an enhancer, enhancer function would be difficult to reconcile with *Jpx*'s *trans* effects.

Jpx's *trans*-acting property might be better explained by a diffusible ncRNA. To distinguish RNA-based mechanisms from those of DNA, chromatin, and/or transcriptional activity, we used shRNA to deplete *Jpx* RNA after it is transcribed and to knock down both *Jpx* alleles. We generated clones of wildtype female ES cells carrying one of three *Jpx*-specific shRNAs directed against nonpolymorphic regions of exon 1 (Fig. 4A: shRNA-A, -B, -C) and analyzed 2–3 independent clones with good knockdown efficiency for each (e.g., shRNA-A1, -A2, -A3). Controls carrying scrambled shRNA (Scr) were generated and analyzed in parallel. Using qRT-PCR with primer pairs positioned in exon 1, we observed 70–90% depletion of *Jpx* RNA (Fig. 4B). Allele-specific RT-PCR showed that 129 and *castaneus* alleles were symmetrically targeted (Fig. 4C). Because all clones behaved similarly, results are shown for representative clones.

Phenotype analysis indicated that all knockdown clones recapitulated ΔJpx . Knockdown clones grew indistinguishably from wildtype on d0 and only lost viability upon differentiation (Fig. 4D, E). Between d0–d4, EB formed by shRNA clones were inferior in size and quality to those of wildtype and Scr control (Fig. 4E). Between d4–d12, knockdown EB showed poor outgrowth and underwent massive cell death at magnitudes comparable to those for $\Delta Jpx/+$ cells (Fig. 4D, E). *Xist* RNA FISH indicated a deficiency of *Xist*⁺ cells in differentiating knockdown clones, (Fig. 4F, G). Similarly, qRT-PCR demonstrated significantly lower *Xist* levels when *Jpx* RNA was knocked down by *Jpx*-specific shRNAs (Fig. 4H). These data showed that targeting both *Jpx* alleles for post-transcriptional RNA degradation recapitulates the heterozygous deletion.

In $\Delta Jpx/+$ cells, only 10–20% of *Jpx* RNA remained, though the *castaneus* allele was not deleted. To determine the consequences of further *Jpx* deletion, we introduced shRNA-C into the heterozygous cells (1F8) and depleted *Jpx* RNA by another ~50% (Fig. 4I). Further depletion did not worsen the already severe phenotype, as *Xist* upregulation remained similarly compromised and EB viability remained poor (Fig. 4I), possibly because *Jpx* was

already largely abrogated. Thus, post-transcriptional depletion of *Jpx* RNA achieves the equivalent of the *Jpx*^{-/-} state (~10% residual RNA) and argues that *Jpx* acts as a long ncRNA.

***Jpx* has a mild *cis* preference**

While ΔJpx eliminated almost all female cells during differentiation, a very small subset persisted past d20 and continued to proliferate, indicating that rare cells might bypass ΔJpx . To investigate the XCI status of surviving cells, we expanded survivors to d28, performed Xist RNA FISH, and found that Xist induction occurred in almost all survivors (Fig. 5A). To ask which of two *Xist* alleles was upregulated, we performed allele-specific RNA-DNA FISH and observed that *Xist* was induced monoallelically from X¹²⁹ or X^{cas} (Fig. 5B; RNA/DNA FISH showed that >95% of mutant cells are XX; only XX cells were counted). However, X^{cas} was favored by a ratio of 65:35 in d28 survivors (Fig. 5C), indicating that ΔJpx is a disadvantage for the *Xist* allele linked to it. Allele-specific RT-PCR of *Xist*, *Pgk1*, *Mecp2*, and *Hprt* ratios confirmed these findings (Fig. 5D). RNA FISH also demonstrated that Xist upregulation led to silencing of genes *in cis* (Fig. 5E), demonstrating that *Jpx* does not affect gene silencing *per se*. The observed allelic biases were the opposite of wildtype, which ordinarily favors inactivating X¹²⁹ due to the strain-specific *Xce* modifier (Cattanach and Isaacson, 1967). Thus, although *trans*-acting, *Jpx* has a measurable *cis* preference that is uncovered only in rare female survivors (Fig. 5F).

Antagonism between *Tsix* and *Jpx* in the control of *Xist*

Several models for *Xist* regulation postulate a balancing act between positive and negative factors (Lee and Lu, 1999; Lee, 2005; Monkhorst et al., 2008; Navarro et al., 2008; Donohoe et al., 2009; Starmer and Magnuson, 2009; Ahn and Lee, 2010). *Xite* and *Tsix* clearly reside in the repressive regulatory arm (Lee and Lu, 1999; Sado et al., 2001; Ogawa and Lee, 2003). ΔJpx 's phenotype suggests that *Jpx* may reside in a parallel, opposing arm. To test the idea of *Jpx* and *Tsix* antagonism, we targeted the *Tsix*^{TST} mutation (Ogawa et al., 2008) into $\Delta Jpx/+$ cells to truncate *Tsix* RNA on the chromosome bearing ΔJpx (Fig. 6A). Targeting was confirmed by Southern blot analysis and allele-specific genotyping (Fig. 6B and data not shown). Intriguingly, truncating *Tsix* almost completely restored viability and differentiation of $\Delta Jpx/+$ cells. Cell death analysis showed that two independently derived double mutants, 1F8-S1 and 1F8-S2, have reduced cell death between d6–d12 when compared to the single mutant (Fig. 6C). Cell death was comparable to that of wildtype EB, though significantly higher between d4–d6. Furthermore, unlike single mutants, double mutants exhibited normal EB morphology and outgrowth (Fig. 6D) and RNA FISH showed restoration of *Xist* upregulation and kinetics (Fig. 6E, F). These results demonstrate that *Tsix*^{TST} suppresses ΔJpx .

We next asked how allelic choice was further affected in *Jpx-Tsix* double mutants. Single mutations both skew XCI ratios, but the polarity is opposite: *Tsix*^{TST/+} cells exclusively inactivate X¹²⁹ (Ogawa et al., 2008), whereas $\Delta Jpx/+$ survivors preferentially inactivate X^{cas} (Fig. 5). In the double mutant, allele-specific RT-PCR for *Xist*, *Pgk1*, and *Mecp2* expression revealed *Tsix*'s dominance over *Jpx* (Fig. 6G). Abrogating *Tsix* RNA not only overcame the block to transactivate *Xist*, but also skewed choice to favor X¹²⁹. Therefore, when *Tsix* RNA is eliminated, the linked *Xist* allele is induced despite a *Jpx* deficiency. To determine whether further reduction of *Jpx* by shRNA knockdown affected the rescue, we introduced shRNA-C into the double mutant but did not observe additional effects on *Xist* expression or cell viability (Fig. 6H, I).

In principle, the rescue of ΔJpx by *Tsix*^{TST} could be interpreted in two ways. One idea is that *Tsix* and *Jpx* reside a single genetic pathway in which *Jpx* occurs upstream of *Tsix* and

controls *Xist* expression by suppressing *Tsix*'s repressive effect on *Xist*. We do not favor this idea, given that deleting *Jpx* did not affect *Tsix* levels in male cells (Fig. S1H). Moreover, the *Tsix-Jpx* double mutant was not identical in phenotype to *Tsix^{TST}*, as the double mutant still demonstrated elevated cell death at early timepoints in spite of rescuing *Xist* expression (Fig. 6C). Thus, we believe that the data collectively argue for parallel pathways in which *Tsix* and *Jpx* independently control *Xist* transcription. In this scenario, how can *Xist* be induced in double mutants? One possibility is that residual *Jpx* levels from X^{cas} were sufficient to activate *Xist in trans*. This alone cannot explain the rescue, however, as residual *Jpx* from X^{cas} could not upregulate *Xist* at all in $\Delta Jpx/+$ cells (Fig. 2D, F, G). We propose that eliminating the negative arm of regulation (via *Tsix^{TST}*) created a hyper-permissive state for *Xist* upregulation in which even very low *Jpx* expression might be sufficient to induce *Xist* expression.

DISCUSSION

Our work demonstrates that *Xist* is controlled by two parallel RNA switches – *Tsix* for Xa and *Jpx* for Xi. Whereas *Tsix* represses *Xist* on Xa, *Jpx* activates *Xist* on Xi. How *Jpx* RNA transactivates *Xist* is yet to be determined, but it is intriguing that expression of one long ncRNA would be controlled by another. Recapitulation of the knockout by post-transcriptional knockdown of *Jpx* implies that the activator acts as an RNA. Unlike other ncRNAs of the *Xic*, *Jpx* is *trans*-acting and diffusible. Indeed, autosomally expressed *Jpx* RNA can rescue the X-linked ΔJpx defect. We cannot exclude the possibility that *Jpx* also acts as an enhancer, though our reporter assay did not uncover such a property (Fig. S4). Interestingly, 3C analysis previously revealed close chromatin contact between the 5' ends of *Jpx* and *Xist in cis* (Tsai et al., 2008). Their physical proximity may underlie *Jpx*'s preference for the linked *Xist* allele (Fig. 5), as a diffusion-limited *Jpx* RNA would be expected to preferentially bind the *Xist* allele closer to it.

Our findings place *Jpx*'s function in an epistatic context (Fig. 7A). Prior work has proposed that *Xite* and *Tsix* reside at the top of the repressive pathway, controlling XCI counting and choice by inducing homologous chromosome pairing through Oct4 (Bacher et al., 2006; Xu et al., 2006; Donohoe et al., 2009). X-X pairing would play an essential role in breaking epigenetic symmetry by shifting the binding of *Tsix*- and *Xite*-associated transcription factors from both X's to the future Xa (Xu et al., 2006; Nicodemi and Prisco, 2007; Donohoe et al., 2009; Lee, 2009). Retained transcription factors would then sustain *Xite* and *Tsix* expression and block *Xist* activation on Xa (Stavropoulos et al., 2001; Ogawa and Lee, 2003), in part by interfering with the action of RepA RNA and Polycomb proteins (Sun et al., 2006; Zhao et al., 2008).

Work from the current study supports the existence of a parallel, but activating pathway for establishment of Xi. *Jpx* resides in this pathway (Fig. 7A). The RNA is upregulated 10- to 20-fold during ES differentiation and leads to monoallelic *Xist* induction in female cells. The collective evidence suggests that *Jpx* and RepA RNA collaborate to transcriptionally activate *Xist*. In this model, loss of *Tsix* expression on the future Xi would enable the RepA-Polycomb complex to load onto the *Xist* chromatin and trimethylate H3-K27 on the *Xist* promoter (Zhao et al., 2008), creating a permissive state in which *Jpx* RNA could transactivate *Xist*.

In male cells, *Jpx* upregulation does not result in *Xist* induction on the single X – similar to the Xa of female cells. As would be the case for the female Xa, persistence of *Tsix* in male cells overrides *Jpx* by recruiting silencers to the *Xist* promoter (Navarro et al., 2005; Sado et al., 2005; Sun et al., 2006). In the context of *Tsix* regulation, DNA methylation and RNAi have been invoked in *Xist* silencing (Norris et al., 1994; Ariel et al., 1995; Zuccotti and

Monk, 1995; Sado et al., 2005; Sun et al., 2006; Ogawa et al., 2008). By this model, female cells deficient for *Jpx* would be unaffected on d0 because *Jpx* is normally not induced until cell differentiation and the onset of XCI. Once induced, *Jpx* RNA remains at high levels in somatic cells (Fig. 1), implying that continued presence of the activator may be necessary for life-long *Xist* expression in the female. *Jpx* may also play other roles during development, given that the *Tsix-Jpx* double mutant rescues *Xist* expression but does not fully rescue cell death (Fig. 6).

In conclusion, our study identifies *Jpx* as an RNA-based activator of *Xist* and supports a dynamic balance of activators and repressors for XCI control. The fate of *Xist* appears to be determined by a series of *Xic*-encoded RNA switches, reinforcing the idea that long ncRNAs may be ideally suited to epigenetic regulation involving allelic and locus-specific control (Lee, 2009). Future work will help elucidate why the *Xic*, once protein-coding, was replaced in recent evolutionary history by noncoding genes.

MATERIALS AND METHODS

Construction of ΔJpx cell lines

Male (J1) and female (16.7) ES cell lines, culture condition, and cell differentiation protocols have been described (Lee and Lu, 1999). To generate ΔJpx , a 5' homology arm (6.5 kb BstZ17I-BglI of *Jpx*) was cloned into the NotI site of vector, PgcNeo2LoxDTA. To the resulting vector was cloned the 3' arm (6.19 kb AvrII-PstI fragment) into the NheI-SalI site, yielding a 5.17 kb deletion. The targeting construct was linearized with XhoI and electroporated. For screening, ~2000 male and ~2500 female G418-resistant clones were picked, and 4 male and 5 female independent knockout clones were analyzed. To excise the *Neo* selection marker, a Cre plasmid (pMC-CreN) was introduced and G418-sensitive colonies identified. Homologous targeting was confirmed by genomic Southern blots using 5' and 3' external probes, as well as internal probes to rule out ectopic integrations. The templates for 5' and 3' external probes were PCR products generated using primers: GAGCTCTGAGACACAGCGCAA and GCCAAAGGGGTTGTCATCTATG for the 5' probe (nt 84779–85380 of GenBank sequence AJ421479); and GCCCAGGAAGTGGATTTTAGCACA and TGCTTATGGACGATCAAAGTGCC for the 3' probe (nt 104761–105450 of AJ421479). To determine which allele was targeted in females, we carried out allele-specific PCR analysis based on a Nla-III polymorphic site at nt 95,738 (GenBank sequence AJ421479) within *Jpx* (CATG for the 129; CAAG for *castaneus*). Genomic DNA was amplified by primer pairs, *JpxUp* (CGGCGTCCACATGTATACGTCC) and *JpxLo* (TAGGAATGAGCCTCCCCAGCCT) (Chureau et al., 2002), to generate a 329bp product (nt 95598–95926 of GenBank AJ421479), which was then digested with Nla-III to yield 142, 95, 83 and 9-bp fragments for 129 and 237, 83, and 9-bp fragments for *castaneus*. All female clones showed targeting of the 129 allele.

Generation of transgenic *Jpx* cell lines

A 90-kb BAC transgene containing full-length *Jpx* (and no other known transcribed sequences) and a *Neo* resistance marker was made by ET-cloning (Yang and Seed, 2003) from BAC clone 399K20 (Invitrogen). Ten million 1F8 cells ($\Delta Jpx/+$) were electroporated with 20 μ g linearized BAC DNA and cultured under G418 selection (250 μ g/ml). Two G418-resistant clones (TgB2 and TgB3) were picked on d8 and expanded for analysis.

Generation of *Tsix^{TST} $\Delta Jpx/+$* ES cells

The *Tsix^{TST}* truncation vector has been described (Ogawa et al., 2008). The $\Delta Jpx/+$ female line, 1F8, was electroporated with the *Tsix^{TST}* vector, 96 clones were picked after puromycin

selection, and targeting into X^{129} was determined by Southern blot analysis and allele-specific PCR, as described (Ogawa et al., 2008). Two independent clones, 1F8-S1 and 1F8-S2, were analyzed in parallel.

Generation of Jpx knockdown clones

To generate three shRNA knockdown plasmids, three nonpolymorphic sequences from *Jpx* exon 1 were inserted into the *EcoRI* and *NheI* site of pLKO1 (Addgene):

shRNA-A: 5'-
CCGGCACCAGGCTTCTGTAAGTTATCTCGAGATAAGTTACAGAAGCCTGGTG
TTTTTG-3'

shRNA-B: 5'-
CCGGTAGAGGATGACTTAATAAGGACTCGAGTCCTTATTAAGTCATCCTCTA
TTTTTG-3'

shRNA-C: 5'-
CCGGGGCGTCCACATGTATACGTCCCTCGAGGGACGTATACATGTTCGACGC
CTTTTTG-3'

16.7 cells were electroporated with either Jpx-specific or a scrambled (Scr) shRNA vector and selected with puromycin for stable integration. Multiple independent clones were picked (24 for shRNA-A, 24 for shRNA-B, and 48 for shRNA-C) and tested for Jpx knockdown efficiency by qRT-PCR (see **Quantitative RT-PCR**). We analyzed 2–3 independent clones for each.

RNA and DNA FISH

FISH protocols and probes (*Xist*, *Pgk1*) have been described (Lee and Lu, 1999; Stavropoulos et al., 2001). The *Jpx* probe is a 3.7 kb fragment (nt 93362–97039 of GenBank AJ421479) within the deleted region that was cloned into pCR-Blunt II-Topo vector (Invitrogen) for Nick translation. For two-color strand-specific RNA FISH, an FITC-labelled *Xist* riboprobe cocktail was generated by in vitro transcription (MAXIscript kit, Ambion) to detect the *Xist* strand, and *Tsix* was detected by Cy3-labelled pCC3, a 5' *Tsix* probe that does not overlap *Xist* (Lee et al., 1999a; Ogawa and Lee, 2003).

Quantitative RT-PCR

Real-time PCR for *Xist*, *Tsix*, and *Jpx* was performed under the following conditions: 95°C 3min; 95°C 10sec, 60°C 20sec, 72°C 20sec, for a total of 40 cycles, and 72°C 5min. Melting curves for primer pairs were determined by increasing temperatures from 60°C to 95°C at 0.5°C interval for 5sec. Primers for *Xist* qRT-PCR were NS66 and NS33, and for *Tsix* NS18 and NS19 (Stavropoulos et al., 2001). Primers for *Jpx* were *e1-F*, GCACCACCAGGCTTCTGTAAC, and *e1-R*, GGGCATGTTTCATTAATTGGCCAG.

Allele-specific RT-PCR

Allele-specific RT-PCR was performed as described (Stavropoulos et al., 2001; Ogawa and Lee, 2003). Total RNA was extracted by Trizol (Invitrogen) and DNA was removed with DNase I treatment (Ambion). Reverse transcription was then performed with SuperScript III First Strand Synthesis System (Invitrogen). Allele-specific primers were: NS66 and NS33 for *Xist* (Stavropoulos et al., 2001), NS18 and NS19 for *Tsix* (Stavropoulos et al., 2001), NS43 and NS44 for *Mecp2* (Ogawa and Lee, 2003), KH106 and KH107 for *Pgk1* (Huynh and Lee, 2003), NS41 and NS70 for *Hprt* (Stavropoulos et al., 2001). Southern blot was carried out using nested primers as probes as referenced above: XSP1 for *Xist*, NS19 for *Tsix*, NS65 for *Mecp2*, KH106 for *Pgk1*, and NS59 for *Hprt*. For *Jpx* allele-specific RT-

PCR, Jpx cDNA was amplified with JpxLow and JpxUp to generate a 329bp product, which was digested with NlaIII. End-labeled oligonucleotide, Jpx-P1, GGTGATGTGGGCACTGATCACTCATC, was used as southern probe to recognize both castaneus specific 237 bp and 129 specific 142 bp band. All allelic signals were then quantitated by phosphorimaging.

Luciferase assay

Promoterless pGL4.19 (Promega) was used to construct luciferase vectors. To generate Jpx-pGL4, a 5.29 kb fragment (nt 92711–98009 of AJ421479), corresponding to the knockout region (promoter, CpG island, and exons 1–2), was cloned into the multiple cloning site. To construct Xist-pGL4, a 4.43 kb fragment (nt104971–109403 of AJ421479), containing the 500-bp region upstream of *Xist*'s start site and the proximal 4 kb of exon 1, was cloned similarly. Jpx-Xist-pGL4 was constructed by inserting the 5.29 kb Jpx fragment upstream of Xist in Xist-pGL4 vector. Vectors were individually electroporated into female ES cells, and 200–300 stably transfected clones from each vector were pooled and subjected to luciferase assay at different differentiation timepoints. qRT-PCR for luciferase was performed using primers, Luc-F1, CAGCGCCATTCTACCCACTCG, and Luc-R1, GCTTCTGCCAGCCGAACGC. Beta-actin was amplified as the internal control.

Cell death analysis

Cell death assays were performed as described (Stavropoulos et al., 2001). Briefly, on d0, both supernatant and attached ES cells were collected and stained with Trypan blue dye (Sigma). On other time points, both supernatant and floating embryoid bodies (EBs on d4) or attached EBs (day6 and onward) were collected and stained with Trypan blue. The ratios of dead cells (blue) to total cells (i.e., blue dead cells + clear viable cells) were calculated and plotted as a function of time. Each sample was counted in duplicate or triplicate.

Supplementary Material

Refer to Web version on PubMed Central for supplementary material.

Acknowledgments

We thank Y. Jeon for providing Xist riboprobes, and A. Chess, D. Lessing, B. Payer, and S. Pinter for critical reading of the manuscript and all members of the laboratory for their helpful input throughout this project. This work was funded by NIH grants K08-HD053824 to D.T. and RO1-GM58839 to J.T.L. J.T.L. is also an Investigator of the Howard Hughes Medical Institute.

References

- Ahn JY, Lee JT. Retinoic acid accelerates downregulation of the Xist repressor, Oct4, and increases the likelihood of Xist activation when Tsix is deficient. *BMC Dev Biol.* 2010; 10:90. [PubMed: 20727175]
- Ariel M, Robinson E, McCarrey JR, Cedar H. Gamete-specific methylation correlates with imprinting of the murine Xist gene. *Nat Genet.* 1995; 9:312–315. [PubMed: 7773295]
- Bacher CP, Guggiari M, Brors B, Augui S, Clerc P, Avner P, Eils R, Heard E. Transient colocalization of X-inactivation centres accompanies the initiation of X inactivation. *Nat Cell Biol.* 2006; 8:293–299. [PubMed: 16434960]
- Brockdorff N, Ashworth A, Kay GF, McCabe VM, Norris DP, Cooper PJ, Swift S, Rastan S. The product of the mouse Xist gene is a 15 kb inactive X-specific transcript containing no conserved ORF and located in the nucleus. *Cell.* 1992; 71:515–526. [PubMed: 1423610]
- Brown CJ, Hendrich BD, Rupert JL, Lafreniere RG, Xing Y, Lawrence J, Willard HF. The human XIST gene: analysis of a 17 kb inactive X-specific RNA that contains conserved repeats and is highly localized within the nucleus. *Cell.* 1992; 71:527–542. [PubMed: 1423611]

- Brown CJ, Lafreniere RG, Powers VE, Sebastio G, Ballabio A, Pettigrew AL, Ledbetter DH, Levy E, Craig IW, Willard HF. Localization of the X inactivation centre on the human X chromosome in Xq13. *Nature*. 1991; 349:82–84. [PubMed: 1985270]
- Cattanach BM, Isaacson JH. Controlling elements in the mouse X chromosome. *Genetics*. 1967; 57:331–346. [PubMed: 5584570]
- Chow JC, Hall LL, Clemson CM, Lawrence JB, Brown CJ. Characterization of expression at the human XIST locus in somatic, embryonal carcinoma, and transgenic cell lines. *Genomics*. 2003; 82:309–322. [PubMed: 12906856]
- Chureau C, Prissette M, Bourdet A, Barbe V, Cattolico L, Jones L, Eggen A, Avner P, Duret L. Comparative sequence analysis of the X-inactivation center region in mouse, human, and bovine. *Genome Res*. 2002; 12:894–908. [PubMed: 12045143]
- Clemson CM, Hall LL, Byron M, McNeil J, Lawrence JB. The X chromosome is organized into a gene-rich outer rim and an internal core containing silenced nongenic sequences. *Proc Natl Acad Sci U S A*. 2006; 103:7688–7693. [PubMed: 16682630]
- Davidow LS, Breen M, Duke SE, Samollow PB, McCarrey JR, Lee JT. The search for a marsupial XIC reveals a break with vertebrate synteny. *Chromosome Res*. 2007; 15:137–146. [PubMed: 17333538]
- Donohoe ME, Silva SS, Pinter SF, Xu N, Lee JT. The pluripotency factor Oct4 interacts with Ctf and also controls X-chromosome pairing and counting. *Nature*. 2009; 460:128–132. [PubMed: 19536159]
- Duret L, Chureau C, Samain S, Weissenbach J, Avner P. The Xist RNA gene evolved in eutherians by pseudogenization of a protein-coding gene. *Science*. 2006; 312:1653–1655. [PubMed: 16778056]
- Hoki Y, Kimura N, Kanbayashi M, Amakawa Y, Ohhata T, Sasaki H, Sado T. A proximal conserved repeat in the Xist gene is essential as a genomic element for X-inactivation in mouse. *Development*. 2009; 136:139–146. [PubMed: 19036803]
- Hore TA, Koina E, Wakefield MJ, Marshall Graves JA. The region homologous to the X-chromosome inactivation centre has been disrupted in marsupial and monotreme mammals. *Chromosome Res*. 2007; 15:147–161. [PubMed: 17333539]
- Huynh KD, Lee JT. Inheritance of a pre-inactivated paternal X chromosome in early mouse embryos. *Nature*. 2003; 426:857–862. [PubMed: 14661031]
- Johnston CM, Newall AE, Brockdorff N, Nesterova TB. Enox, a novel gene that maps 10 kb upstream of Xist and partially escapes X inactivation. *Genomics*. 2002; 80:236–244. [PubMed: 12160738]
- Jonkers I, Barakat TS, Achame EM, Monkhorst K, Kenter A, Rentmeester E, Grosveld F, Grootegoed JA, Gribnau J. RNF12 is an X-Encoded dose-dependent activator of X chromosome inactivation. *Cell*. 2009; 139:999–1011. [PubMed: 19945382]
- Koerner MV, Pauler FM, Huang R, Barlow DP. The function of non-coding RNAs in genomic imprinting. *Development*. 2009; 136:1771–1783. [PubMed: 19429783]
- Lee JT. Disruption of imprinted X inactivation by parent-of-origin effects at Tsix. *Cell*. 2000; 103:17–27. [PubMed: 11051544]
- Lee JT. Regulation of X-chromosome counting by Tsix and Xite sequences. *Science*. 2005; 309:768–771. [PubMed: 16051795]
- Lee JT. Lessons from X-chromosome inactivation: long ncRNA as guides and tethers to the epigenome. *Genes Dev*. 2009; 23:1831–1842. [PubMed: 19684108]
- Lee JT, Davidow LS, Warshawsky D. Tsix, a gene antisense to Xist at the X-inactivation centre. *Nat Genet*. 1999a; 21:400–404. [PubMed: 10192391]
- Lee JT, Lu N. Targeted mutagenesis of Tsix leads to nonrandom X inactivation. *Cell*. 1999; 99:47–57. [PubMed: 10520993]
- Lee JT, Lu N, Han Y. Genetic analysis of the mouse X inactivation center defines an 80-kb multifunction domain. *Proc Natl Acad Sci U S A*. 1999b; 96:3836–3841. [PubMed: 10097124]
- Lucchesi JC, Kelly WG, Panning B. Chromatin remodeling in dosage compensation. *Annu Rev Genet*. 2005; 39:615–651. [PubMed: 16285873]
- Luikenhuis S, Wutz A, Jaenisch R. Antisense transcription through the Xist locus mediates Tsix function in embryonic stem cells. *Mol Cell Biol*. 2001; 21:8512–8520. [PubMed: 11713286]

- Lyon MF. Gene action in the X-chromosome of the mouse (*Mus musculus* L.). *Nature*. 1961; 190:372–373. [PubMed: 13764598]
- Marahrens Y, Panning B, Dausman J, Strauss W, Jaenisch R. Xist-deficient mice are defective in dosage compensation but not spermatogenesis. *Genes Dev*. 1997; 11:156–166. [PubMed: 9009199]
- Mercer TR, Dinger ME, Mattick JS. Long non-coding RNAs: insights into functions. *Nat Rev Genet*. 2009; 10:155–159. [PubMed: 19188922]
- Monk M, Harper MI. Sequential X chromosome inactivation coupled with cellular differentiation in early mouse embryos. *Nature*. 1979; 281:311–313. [PubMed: 551278]
- Monkhorst K, Jonkers I, Rentmeester E, Grosveld F, Gribnau J. X inactivation counting and choice is a stochastic process: evidence for involvement of an x-linked activator. *Cell*. 2008; 132:410–421. [PubMed: 18267073]
- Morey C, Navarro P, Debrand E, Avner P, Rougeulle C, Clerc P. The region 3' to Xist mediates X chromosome counting and H3 Lys-4 dimethylation within the Xist gene. *Embo J*. 2004; 23:594–604. [PubMed: 14749728]
- Namekawa SH, Payer B, Huynh KD, Jaenisch R, Lee JT. Two-step imprinted X inactivation: repeat versus genic silencing in the mouse. *Mol Cell Biol*. 2010; 30:3187–3205. [PubMed: 20404085]
- Navarro P, Chambers I, Karwacki-Neisius V, Chureau C, Morey C, Rougeulle C, Avner P. Molecular coupling of Xist regulation and pluripotency. *Science*. 2008; 321:1693–1695. [PubMed: 18802003]
- Navarro P, Pichard S, Ciaudo C, Avner P, Rougeulle C. Tsix transcription across the Xist gene alters chromatin conformation without affecting Xist transcription: implications for X-chromosome inactivation. *Genes Dev*. 2005; 19:1474–1484. [PubMed: 15964997]
- Nicodemi M, Prisco A. Symmetry-breaking model for X-chromosome inactivation. *Phys Rev Lett*. 2007; 98:108104. [PubMed: 17358571]
- Norris DP, Patel D, Kay GF, Penny GD, Brockdorff N, Sheardown SA, Rastan S. Evidence that random and imprinted Xist expression is controlled by preemptive methylation. *Cell*. 1994; 77:41–51. [PubMed: 8156596]
- Ogawa Y, Lee JT. Xite, X-inactivation intergenic transcription elements that regulate the probability of choice. *Mol Cell*. 2003; 11:731–743. [PubMed: 12667455]
- Ogawa Y, Sun BK, Lee JT. Intersection of the RNA Interference and X-Inactivation Pathways. *Science*. 2008; 320:1336–1341. [PubMed: 18535243]
- Ohhata T, Hoki Y, Sasaki H, Sado T. Tsix-deficient X chromosome does not undergo inactivation in the embryonic lineage in males: implications for Tsix-independent silencing of Xist. *Cytogenet Genome Res*. 2006; 113:345–349. [PubMed: 16575199]
- Ohhata T, Hoki Y, Sasaki H, Sado T. Crucial role of antisense transcription across the Xist promoter in Tsix-mediated Xist chromatin modification. *Development*. 2008; 135:227–235. [PubMed: 18057104]
- Payer B, Lee JT. X Chromosome Dosage Compensation: How Mammals Keep the Balance. *Annu Rev Genet*. 2008; 42:733–772. [PubMed: 18729722]
- Penny GD, Kay GF, Sheardown SA, Rastan S, Brockdorff N. Requirement for Xist in X chromosome inactivation. *Nature*. 1996; 379:131–137. [PubMed: 8538762]
- Plath K, Fang J, Mlynarczyk-Evans SK, Cao R, Worringer KA, Wang H, de la Cruz CC, Otte AP, Panning B, Zhang Y. Role of histone H3 lysine 27 methylation in X inactivation. *Science*. 2003; 300:131–135. [PubMed: 12649488]
- Sado T, Hoki Y, Sasaki H. Tsix silences Xist through modification of chromatin structure. *Dev Cell*. 2005; 9:159–165. [PubMed: 15992549]
- Sado T, Wang Z, Sasaki H, Li E. Regulation of imprinted X-chromosome inactivation in mice by Tsix. *Development*. 2001; 128:1275–1286. [PubMed: 11262229]
- Schoeftner S, Sengupta AK, Kubicek S, Mechtler K, Spahn L, Koseki H, Jenuwein T, Wutz A. Recruitment of PRC1 function at the initiation of X inactivation independent of PRC2 and silencing. *Embo J*. 2006; 25:3110–3122. [PubMed: 16763550]
- Shevchenko AI, Zakharova IS, Elisaphenko EA, Kolesnikov NN, Whitehead S, Bird C, Ross M, Weidman JR, Jirtle RL, Karamysheva TV, et al. Genes flanking Xist in mouse and human are

- separated on the X chromosome in American marsupials. *Chromosome Res.* 2007; 15:127–136. [PubMed: 17333537]
- Silva J, Mak W, Zvetkova I, Appanah R, Nesterova TB, Webster Z, Peters AH, Jenuwein T, Otte AP, Brockdorff N. Establishment of histone h3 methylation on the inactive X chromosome requires transient recruitment of Eed-Enx1 polycomb group complexes. *Dev Cell.* 2003; 4:481–495. [PubMed: 12689588]
- Simmler MC, Cunningham DB, Clerc P, Verinat T, Caudron B, Cruaud C, Pawlak A, Szpirer C, Weissenbach J, Claverie JM, et al. A 94 kb genomic sequence 3' to the murine Xist gene reveals an AT rich region containing a new testis specific gene Tsx. *Hum Mol Genet.* 1996; 5:1713–1726. [PubMed: 8922998]
- Starmer J, Magnuson T. A new model for random X chromosome inactivation. *Development.* 2009; 136:1–10. [PubMed: 19036804]
- Stavropoulos N, Lu N, Lee JT. A functional role for Tsix transcription in blocking Xist RNA accumulation but not in X-chromosome choice. *Proc Natl Acad Sci U S A.* 2001; 98:10232–10237. [PubMed: 11481444]
- Sun BK, Deaton AM, Lee JT. A transient heterochromatic state in Xist preempts X inactivation choice without RNA stabilization. *Mol Cell.* 2006; 21:617–628. [PubMed: 16507360]
- Tsai CL, Rowntree RK, Cohen DE, Lee JT. Higher order chromatin structure at the X-inactivation center via looping DNA. *Dev Biol.* 2008; 319:316–425.
- Vigneau S, Augui S, Navarro P, Avner P, Clerc P. An essential role for the DXPas34 tandem repeat and Tsix transcription in the counting process of X chromosome inactivation. *Proc Natl Acad Sci U S A.* 2006; 103:7390–7395. [PubMed: 16648248]
- Wan LB, Bartolomei MS. Regulation of imprinting in clusters: noncoding RNAs versus insulators. *Adv Genet.* 2008; 61:207–223. [PubMed: 18282507]
- Wutz A, Gribnau J. X inactivation Xplained. *Curr Opin Genet Dev.* 2007; 17:387–393. [PubMed: 17869504]
- Wutz A, Rasmussen TP, Jaenisch R. Chromosomal silencing and localization are mediated by different domains of Xist RNA. *Nat Genet.* 2002; 30:167–174. [PubMed: 11780141]
- Xu N, Tsai CL, Lee JT. Transient homologous chromosome pairing marks the onset of X inactivation. *Science.* 2006; 311:1149–1152. [PubMed: 16424298]
- Yang Y, Seed B. Site-specific gene targeting in mouse embryonic stem cells with intact bacterial artificial chromosomes. *Nat Biotechnol.* 2003; 21:447–451. [PubMed: 12627171]
- Zhao J, Sun BK, Erwin JA, Song JJ, Lee JT. Polycomb proteins targeted by a short repeat RNA to the mouse X chromosome. *Science.* 2008; 322:750–756. [PubMed: 18974356]
- Zuccotti M, Monk M. Methylation of the mouse Xist gene in sperm and eggs correlates with imprinted Xist expression and paternal X inactivation. *Nat Genet.* 1995; 9:316–320. [PubMed: 7773296]

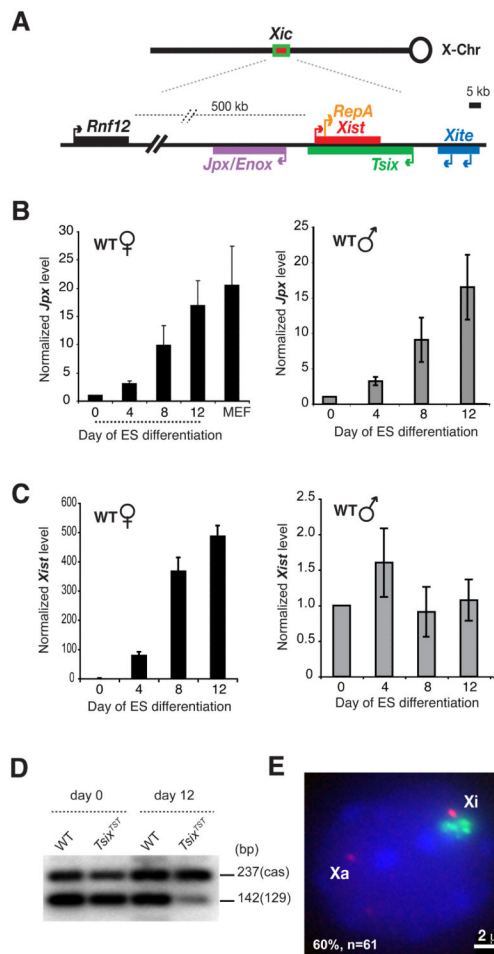


Figure 1. *Jpx* expression increases 10- to 20-fold during ES cell differentiation

(A) The *Xic* and its noncoding genes. *Rnf12* is coding and lies 500 kb away.

(B) Time-course analyses of *Jpx* expression by qRT-PCR in differentiating female and male ES cells. Averages and standard error (S.E.) from three (female) or four (male) independent differentiation experiments are plotted. Values are normalized to *Gapdh* RNA and d0 *Jpx* levels are set to 1.0.

(C) Time-course analyses of *Xist* expression by qRT-PCR in differentiating male and female ES cells. Averages and S.E. from 6 (male) and 3 (female) independent differentiation experiments are plotted. All values are normalized to *Gapdh* RNA and d0 *Xist* is set to 1.0.

(D) Allele-specific RT-PCR analysis of *Jpx* in wildtype and *Tsix*^{TST/+} female ES cells on d0 and d12 of differentiation

(E) RNA FISH indicates that *Jpx* escapes inactivation in 60% of d16 female cells. N=61. *Xist* clouds are present in 98% of cells. *Xist* RNA, green. *Jpx* RNA, red.

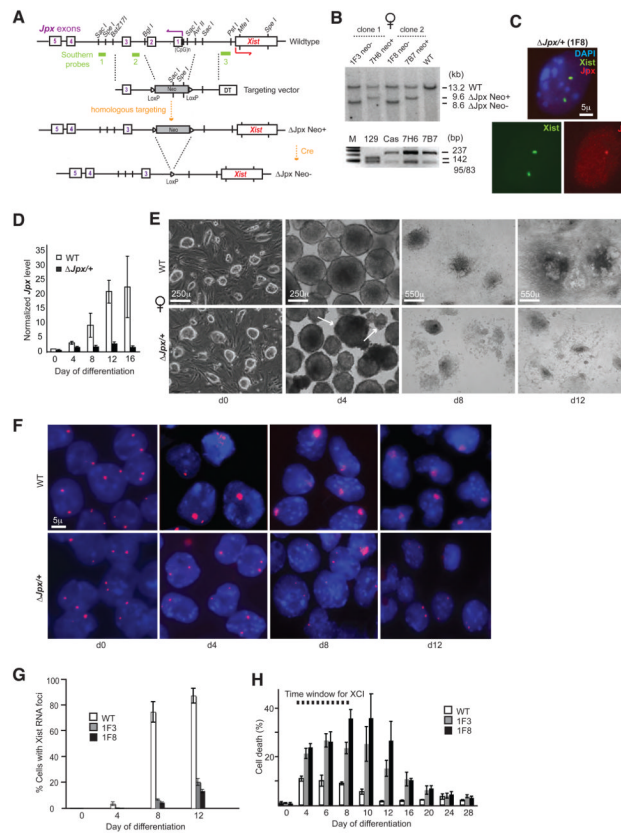


Figure 2. ΔJpx causes loss of XCI and massive cell death in female ES cells

(A) The *Jpx* gene, targeting vector, and products of homologous targeting before and after Cre-mediated excision of the *Neo* positive-selection marker. DT, diphtheria toxin for negative selection. (CpG)_n, CpG island. Numbered boxes represent five *Jpx* exons.

(B) Top panel: Southern analysis of *Sac*I-digested genomic DNA from $\Delta Jpx/+$ and WT female ES cells using probe 1. The *Neo*- female clones, 1F3 and 1F8, were derived from the *Neo*+ 6H7 and 7B7 clones, respectively. Bottom panel: Allele-specific PCR analysis showed that the 129 allele was preferentially targeted over the *M. castaneus* (*cas*) allele. The analysis for *Neo*+ 6H7 and 7B7 clones are shown. M, 100-bp markers.

(C) DNA FISH of $\Delta Jpx/+$ female ES cells. *Xist* probe (pSx9), FITC-labeled. The *Jpx* probe (Cy3-labelled, red) is located in the region of deletion.

(D) Time-course analyses of *Jpx* expression by qRT-PCR in differentiating WT and $\Delta Jpx/+$ female ES cells. Averages and standard errors (S.E.) from three independent differentiation experiments are plotted, with values normalized first to *Gapdh* and then d0 WT *Jpx* levels are set to 1.0.

(E) Brightfield photographs of WT and $\Delta Jpx/+$ female ES cells from d0 to d12 of differentiation. Arrows point to disintegrating, necrotic EBs present in mutant cultures.

(F) RNA FISH to examine the time course of *Xist* upregulation. *Xist* probe, Cy3-labelled pSx9.

(G) Plotted time course of *Xist* upregulation in WT and two $\Delta Jpx/+$ mutants, 1F3 and 1F8. Averages \pm S.E. from 3 independent differentiation experiments are shown. Sample sizes (n): d0, 595–621; d4, 922–1163; d8, 3013–4370; d12, 3272–4794.

(H) Massive cell death in mutant female cells. The Trypan blue staining results of 3 independent differentiation experiments were averaged and plotted with S.E. d0, n=150–800 cells for d0; d4, n=200–500 cells; all other timepoints, n=500–2000 cells.

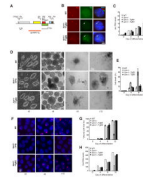


Figure 3. Transgenic *Jpx* rescues ΔJpx in trans

(A) Map of the *Xic* and 90-kb *Jpx* transgene.

(B) Multiprobe DNA FISH to localize *Xist* (pSx9, red) and *Jpx* (BAC, green) in two independent transgenic clones, TgB2 and TgB3. Arrows, *Jpx* transgene.

(C) Time-course analyses of *Jpx* expression by qRT-PCR in differentiating cells of indicated genotype. Averages \pm S.E. from three independent differentiation experiments are plotted. Values are normalized to *Gapdh* RNA and WT d0 *Jpx* level is set to 1.0.

(D) Brightfield photographs of WT and transgenic EB from d0 to d12.

(E) Cell death analysis of WT, knockout, and transgenic EB, performed as above.

(F) RNA FISH to examine the time course of *Xist* upregulation. *Xist* probe, Cy3-labelled pSx9.

(G) Quantitation of WT, knockout, and transgenic EB with *Xist* RNA foci (RNA FISH) from d0–d12.

(H) qRT-PCR of steady state *Xist* levels in WT, knockout, and transgenic EB from d0–d12.

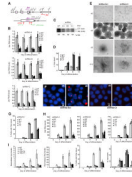


Figure 4. *Jpx* functions as a long ncRNA

(A) A map of the 5' end of *Jpx* showing its exons (purple), shRNA locations, and qPCR primer positions.

(B) Significant knockdown of *Jpx* RNA in 2–3 independent clones for each *Jpx*-specific shRNA, but not in the scrambled shRNA clone (Scr). *Jpx* RNA levels are normalized to WT levels for each day of differentiation. A1–A3 are clones for shRNA-A; B1–B3 for shRNA-B; and C1, C2 for shRNA-C.

(C) Residual *Jpx* RNA was extracted from d8 shRNA clones, A1, B1, and C1, and subjected to allele-specific RT-PCR (Nla-III polymorphism). The gel was blotted and hybridized to an end-labelled oligo. Allelic fractionation shows similar ratios of 129:*castaneus* bands in WT and knockdown clones, suggesting that the shRNAs affected both *Jpx* alleles. Only 10–30% of *Jpx* RNA was left in the knockdowns and therefore the PCR was overcycled to visualize the low residual levels of *Jpx* in the knockdown cells.

(D) Cell death assay shows that loss of *Jpx* RNA reduces cell viability during differentiation. Clones shRNA-C1 and –C2 are shown, but shRNA-A and –B clones also show increased cell death.

(E) Brightfield images show poor EB formation and outgrowth in knockdowns but not Scr control.

(F) Xist RNA FISH shows loss of Xist upregulation when *Jpx* is knocked down using shRNA-C.

(G) Quantitation of the number of cells with Xist RNA clusters from three independent differentiation experiments of control and knockdown clones. Average \pm S.E. shown.

(H) Quantitation of Xist RNA levels in control and knockdown clones from 3 independent differentiation experiments. RNA levels are normalized to d0 WT values. Average \pm S.E. shown. Differentiation of shRNA-A and –B knockdown clones were performed at the same time; therefore, WT and Scr values for shRNA-A and shRNA-B are the same.

(I) *Jpx* knockdown in $\Delta Jpx/+$ cells (1F8) using shRNA-C. Independent clones, C5 and C7, behaved similarly to each other and also to their parent, 1F8, in all assays shown. Average \pm S.E. shown. All values are normalized to d0 WT.

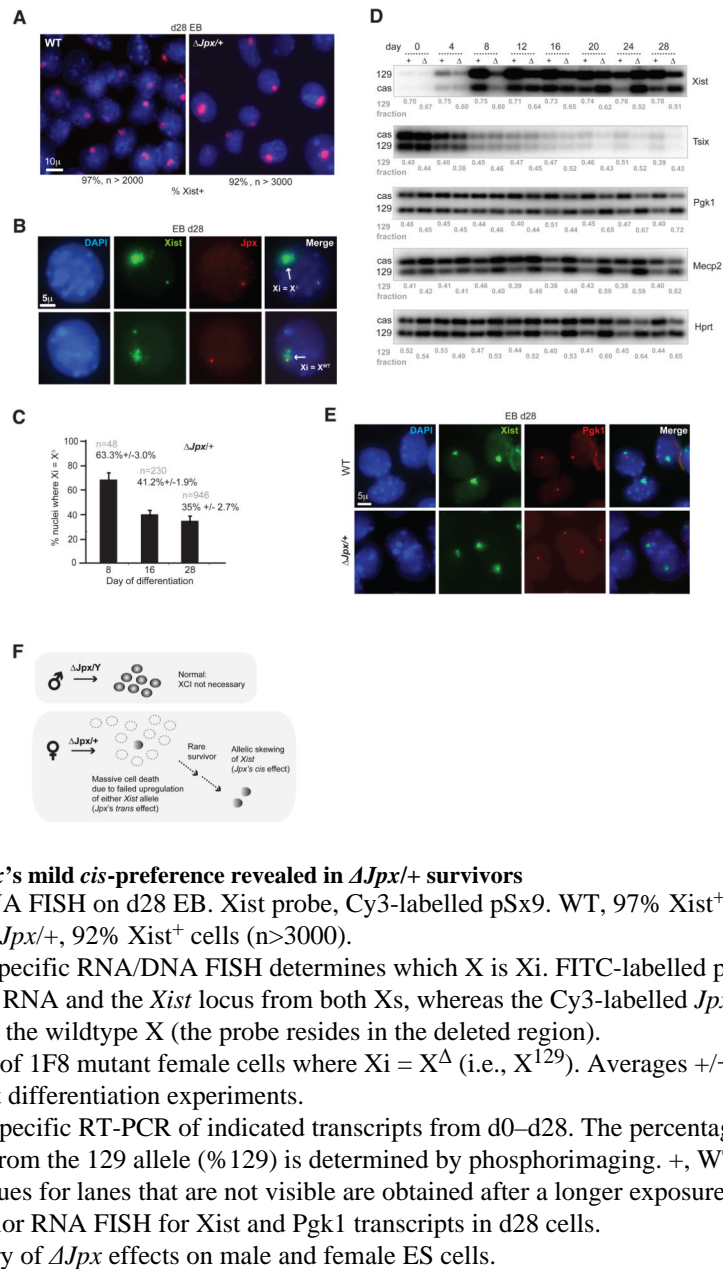


Figure 5. *Jpx*'s mild *cis*-preference revealed in $\Delta Jpx/+$ survivors

(A) Xist RNA FISH on d28 EB. Xist probe, Cy3-labelled pSx9. WT, 97% Xist⁺ cells (n>2000). $\Delta Jpx/+$, 92% Xist⁺ cells (n>3000).

(B) Allele-specific RNA/DNA FISH determines which X is Xi. FITC-labelled pSx9 probe detects Xist RNA and the *Xist* locus from both Xs, whereas the Cy3-labelled *Jpx* probe detects only the wildtype X (the probe resides in the deleted region).

(C) Percent of 1F8 mutant female cells where Xi = X^Δ (i.e., X¹²⁹). Averages ± S.E. from 3 independent differentiation experiments.

(D) Allele-specific RT-PCR of indicated transcripts from d0–d28. The percentage of transcripts from the 129 allele (% 129) is determined by phosphorimaging. +, WT. Δ, 1F8 mutant. Values for lanes that are not visible are obtained after a longer exposure.

(E) Two-color RNA FISH for Xist and Pgf1 transcripts in d28 cells.

(F) Summary of ΔJpx effects on male and female ES cells.

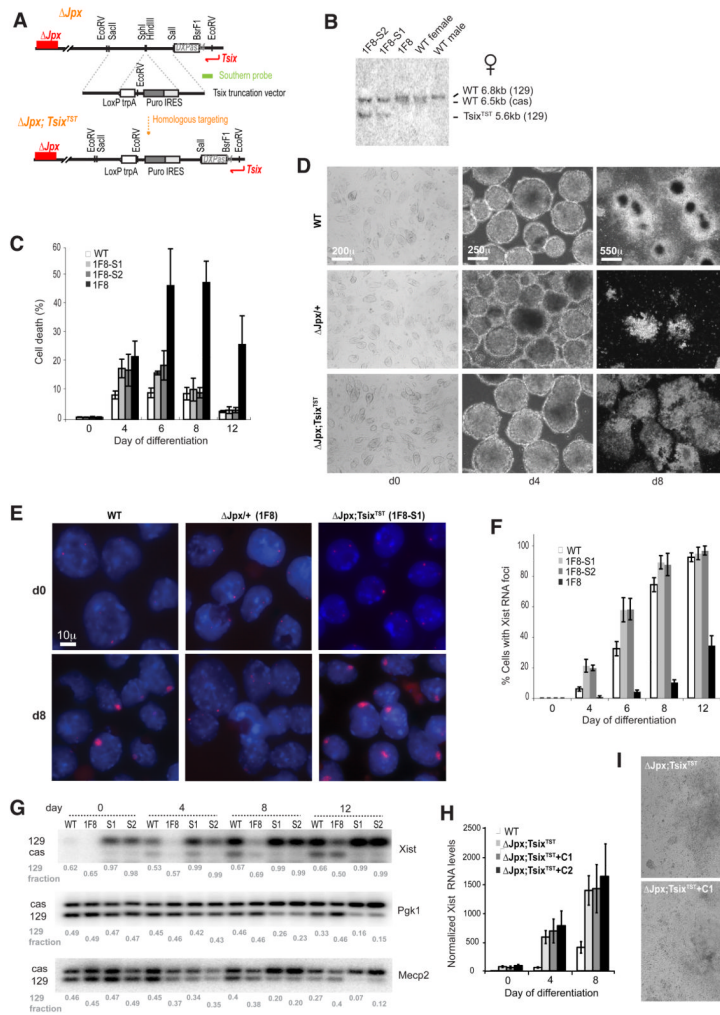


Figure 6. A *Tsix* RNA truncation suppresses ΔJpx
 (A) Targeting the *Tsix* truncation mutation (*Tsix^{TST}*) (Ogawa et al., 2008) to the ΔJpx chromosome in 1F8 female ES cells. *Tsix^{TST}* prematurely terminates *Tsix* at the targeted triple polyA site (trpA) 1 kb downstream of the major *Tsix* promoter. 1F8-S1 and 1F8-S2 are two independently generated double mutant clones. IRES, internal ribosome entry site. Puro, puromycin selection marker.
 (B) Southern analysis using *EcoRV* digestion to confirm targeting. The X^{129} and X^{cas} alleles have a ~300 bp DXPas34 length polymorphism. The X^{129} allele was targeted in both 1F8-S1 and 1F8-S2.
 (C) Cell death analysis shows that *Tsix^{TST}* partially rescues viability of $\Delta Jpx/+$ ES cells.
 (D) Brightfield photographs of wildtype, single, and double mutant female ES cells during differentiation.
 (E) RNA FISH indicating that *Xist* upregulation (large red clouds) is rescued in double mutants.
 (F) *Tsix^{TST}* restores *Xist* induction in $\Delta Jpx/+$ cells. Averages \pm S.D. shown for three independent differentiation experiments.
 (G) The pattern of allelic skewing is reversed in $\Delta Jpx; Tsix^{TST}/+$ cells.
 (H, I) Further depletion of *Jpx* RNA by shRNA-C knockdown in $\Delta Jpx; Tsix^{TST}/+$ cells did not alter the phenotype of the double mutant, as shown by qRT-PCR of *Xist* expression (H)

and by EB outgrowth to d8 (I). *Jpx*; *Tsix*^{TST/+}, 1F8-S2. Two shRNA-C clones derived from 1F8-S2 were examined (C1, C2).

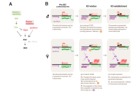


Figure 7. Model and summary

(A) Proposed epistasis model: *Xist* is under positive-negative regulation by noncoding genes. *Xite* and *Tsix* repress *Xist*, whereas *Jpx* and *RepA* activate *Xist*. Arrows, positive relationship. Blunt arrows, negative relationship. *Rnf12* is a coding gene.

(B) Proposed events in male and female ES cells. *Xist* silencers (orange hexagons) include *Dnmt3a* and other chromatin modifications. *Jpx* (purple oval) is depicted as a diffusible transacting RNA. Open lollipops, unmethylated *Xist* promoter. Filled lollipops, methylated *Xist* promoter.